

Investigation on the current-zero characteristic of vacuum circuit breakers



Guowei Ge^{*}, Minfu Liao, Xiongying Duan, Zhihui Huang, Jinqiang Huang, Jiyan Zou

Dalian University of Technology, No.2 Linggong Road, Ganjingzi District, Dalian City, Liaoning Province, 116024, China

ARTICLE INFO

Article history:

Received 8 August 2016

Received in revised form

24 September 2016

Accepted 26 September 2016

Available online 28 September 2016

ABSTRACT

The current-zero characteristic of vacuum circuit breakers (VCBs) has an important influence on the dynamic dielectric recovery and the success of the breaking test. In the paper, the characteristic of the post-arc current, post-arc charge and the post-arc conductance at current-zero is researched to obtain the influence of the arc memory on the current-zero characteristic and the post-arc characteristic. Based on the synthetic test circuit, the test plat of the current-zero characteristic is set up and the test VCB is a transparency vacuum interrupter in order to observe the development and extinguishing process of the vacuum arc by the high speed CMOS camera. The distribution law of post-arc characteristic is gained by measuring and processing the post-arc current. The relationship between the post arc charge and the final position of last cathode spot is investigated. The current-zero characteristic of VCBs supply the base for controlling vacuum arc, improving the breaking capacity, which maybe also useful to VCBs with multi-break.

© 2016 Elsevier Ltd. All rights reserved.

1. Introduction

The VCB is widely used in the medium voltage because of the superior extinguishing ability and the high dielectric recovery strength. However, it is difficult to extend VCBs to high voltage level be limited by the saturation effect which is that the breakdown voltage increases slower even remains unchanged with the increase of the vacuum gap [1]. The current-zero characteristic of VCBs is a key factor to improve the breaking capacity and voltage distribution of multi-break VCBs [2,3].

The current zero characteristic mainly includes the residual plasma in current-zero, the temperature distribution of the anode surface and the post-arc characteristic which is composed of the post-arc current, post-arc conductance and the post-arc charge. There have been a lot of researches on current-zero characteristic. The post-arc sheath growth model is always used to analyze the dynamic dielectric recovery strength as shown in Fig. 1 [4]. At current zero, the residual plasma is composed of ions and electrons, which is electroneutral. The ions continue to move towards the anode because of their inertia while the electrons can adapt their

speed immediately as the electric field is applied. As shown in the Fig. 1, the electrons reduce their speed to zero and then reverse the direction while the transient recovery voltage (*TRV*) is almost zero in this phase. In the second phase, the electrons move towards the new anode and leave an ionic space charge sheath behind. The *TRV* is mainly applied across the sheath. At the third phase, the electrical current drops because that all the electrons have been absorbed by the new anode and the ions current caused by the *TRV* can be negligible [5,6]. The sheath expansion is simulated by a 1D hybrid model of the non-equilibrium post-arc plasma and cathode sheath coupled with a direct simulation Monte Carlo method [7]. The 2d3v model of sheath expansion is established the post-arc decay process [8]. The influence of the electron density and ion temperature on the sheath expansion is investigated by the particle in cell (PIC) simulation [9]. In all of the above simulation, the initial residual plasma and temperature, which is influenced by the arc memory, is set a certain value. The arc memory is the effect of the vacuum arc (including arcing time, arc current, plasma density and temperature) on the current zero characteristic such as the residual plasma, surface temperature of the electrodes, post-arc resistance and the dielectric recovery strength. So the relationship between the arc memory and the current-zero characteristic is needed to be further researched. In the experimental aspect, the distribution of the electron density is gained by the Langmuir probes [10]. The residual plasma is measured by the retarding field analyzer (RFA). The post-

^{*} Corresponding author.

E-mail addresses: geguowei@mail.dlut.edu.cn (G. Ge), mfliao@dlut.edu.cn (M. Liao), dxy@dlut.edu.cn (X. Duan).

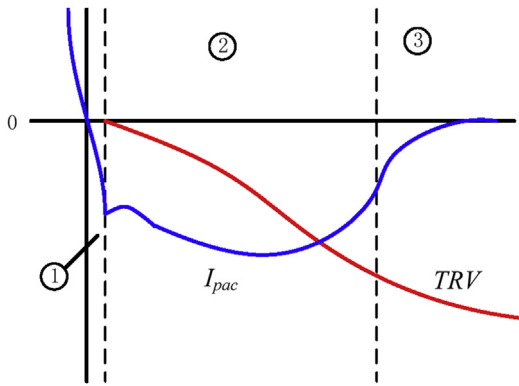


Fig. 1. The post-arc current in VCBs.

arc charge is varied from 9 to 31 μC [11]. The decay process of the anode surface temperature is also researched to gain the optimal magnetic control. The post-arc characteristic such as the post-arc current and charge is always used to indicate the breaking capability of VCBs [12,13].

In conclusion, there are a lot of researches on the current-zero characteristic in previous works. However, there are little researches on the relationship between the arc memory and the current-zero characteristic and the influence of the current-zero characteristic on the post-arc characteristic. In this paper, the test plat is set up to investigate the distribution of the post-arc characteristic by processing the post-arc current. The arc photos are observed by the high speed CMOS camera to analyze the arc memory to the current-zero characteristic such as the post-arc charge. The influence of the final position of the last cathode spot on the post-arc characteristic is obtained.

2. Test configuration

As shown in Fig. 2, the test plat of current-zero characteristic in synthetic circuit is composed of the synthetic test circuit, measuring equipment, the test VCB and the high speed CMOS camera. The maximum capacity of the synthetic test circuit is 110kV/50 kA. The current source consists of L_i and C_i while the voltage source is composed of C_v and L_v . The closing circuit breaker CB is used to introduce the main current while the triggered switch G is used to introduce the high TRV. The post-arc current measure equipment is composed of VI, R_{sh} , SG and CT_1 , which is designed and verified in our previous researches [14,15]. P_{tl} is used to measure the TRV while CT_2 is Rogowski Coil which is used to measure the main current. The VCB is drove by the permanent magnet actuator

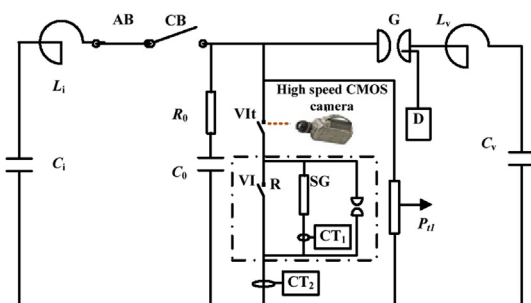


Fig. 2. The test plat of current-zero characteristic in synthetic test circuit.

(PMA) and the vacuum interrupter is transparent in order to observe the development of the vacuum arc by the high speed CMOS camera.

The post arc current is measured by the PACME which is composed of the VCB, protective gap SG, the shunt resistor R_{sh} and CT_1 . As shown in Fig. 3, the VCB is composed of the upper terminal, transparent vacuum interrupter with observing window, the lower terminal, the insulating rod, the PMA and the controller. The detailed parameters can be found in our precious researches [31]. The breaking current is 20 kA while the rated voltage is 10 kV. The high-precision current sensors CT_1 is Tektronix current probe TCP202 whose measuring range, bandwidth and precision is 50 A, 50 MHz and 1% respectively. The resistance of the shunt resistor is 448 m Ω and the maximum current of the shunt resistor is about 30.84 A.

The post-arc current is measured and the vacuum arc photos are observed when the test condition is shown in Table 1. The post-arc conductance and charge can be gained by the formula (1) and (2). The transparent vacuum interrupter is 10kV/20 kA and the contacts are in AMF configuration. The main current is varied from 0 to 15 kA while the TRV is 0–22 kV. When the main current and the TRV is 10 kA and 22 kV respectively, the influence of the arcing time on the post-arc characteristic can be gained. In the condition that the main current and the arcing time are 22 kV and 5 ms respectively, the influence of the main current magnitude on the post-arc characteristic can be obtained. The entire above test is repeatedly conducted in order to gain the distribution law of post-arc characteristic in different condition.

$$G_t = \frac{i_{pac}}{U_{TRV}} \quad (1)$$

$$Q_{pac} = \int_0^t i_{pac} dt \quad (2)$$

3. Experimental result and analysis

3.1. Post-arc characteristic

In the condition that the main current and the TRV are 10 kA and 18 kV respectively, the interrupting test is shown in Fig. 4. The du/dt of the TRV is 4.5 kV/ μs . The period of the half sine-wave is about

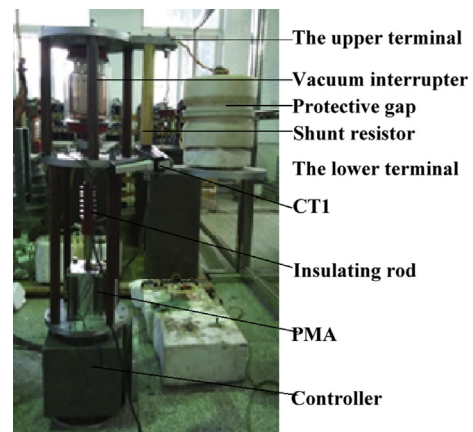


Fig. 3. Prototype of the novel post-arc current measurement equipment (PACME).

Table 1
The configuration of test condition.

I_{main} (kA)	t_{arc} (ms)	U_{TRV} (kV)	du/dt (kV/ μ s)
0	2	0	0
5	3	5	1.25
7.5	4	10	2.5
10	5	15	3.75
12.5	6	18	4.5
15	7	22	5.5

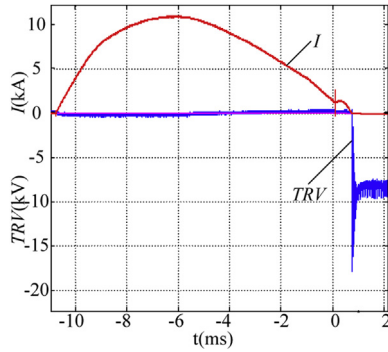


Fig. 4. Waveform of the current and voltage in the interruption.

12 ms. The post-arc current and TRV is shown in Fig. 5 which is the partial enlarged drawing at current-zero. The peak value and the duration of the post-arc current are about 0.6503 A and 4.8 μ s respectively. After the post-arc current approaches to zero in the time of 4.8 μ s, there is a little oscillating current whose frequency is almost same to the TRV, which can be neglected because the magnitude of the oscillating current is very little. When the time is above 4.8 μ s, the post arc current is almost same and the post-arc charge is parallel. The phenomenon indicates that the post-arc characteristic is stable when the time is above 4.8 μ s.

The post-arc conductance and charge is shown in Fig. 6 (a) and (b) by the formula (1) and (2). The post-arc conductance decreases as the time increases when the time is below 4.8 μ s. After that, the post-arc conductance increases with increasing the time. The post-arc impedance is described by the conductance may be not appropriate because that the TRV is high frequency oscillating and it may be correctly with the description of post-arc capacitance. So the initial phase of the post-arc conductance is always more suitable than the post-arc current's peak value because of the divergence of the post-arc current and the typical value in the moment of 0.5 μ s, which is always called $G_{0.5}$, is always used to indicate the post-arc characteristic [4]. The post-arc charge is obtained by time-

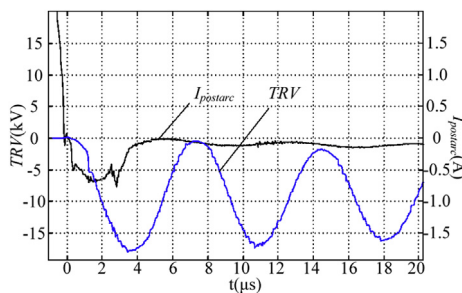


Fig. 5. Post-arc current of VCBs with AMF contacts.

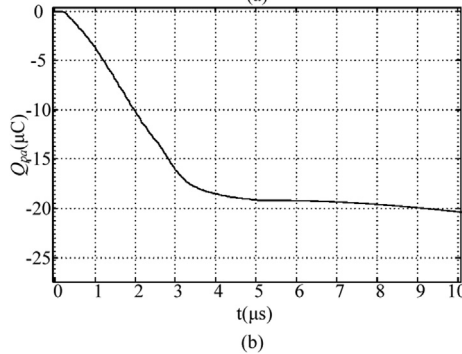
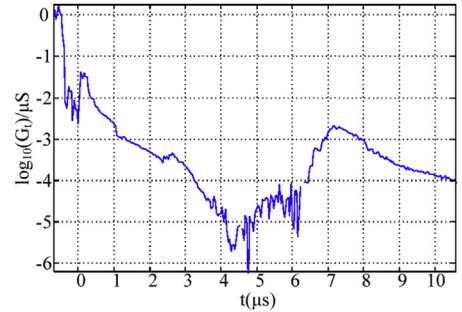


Fig. 6. Post-arc conductance and charge of VCBs with AMF contacts.

integrating the post-arc current, which is more smooth and stable as shown in Fig. 6 (b). The post-arc charge is proportional to the post-arc conductance [16]. However, the post-arc charge is more stable and smooth than post-arc conductance. Therefore, it is optimal to describe the post-arc characteristic by the post-arc charge.

The post arc charge is closely related to the residual plasma in current-zero which is the result of the arc memory in arcing time. The post arc charge is always used to represent the residual plasma in current-zero without considering the field emission caused by the TRV and the neutralization of plasma [12–14]. In the paper, the current zero characteristic is described by the post arc charge.

3.2. The influence of the arcing time

When the main current and the TRV are 10 kA and 18 kV, and the arcing time is varied from 2 ms to 7 ms, the test is repeatedly conducted to gain the influence of the arcing time on the post-arc charge. According to the Fig. 7, the post-arc charge increases as the arcing time increases. The arcing strain (arc memory) increases

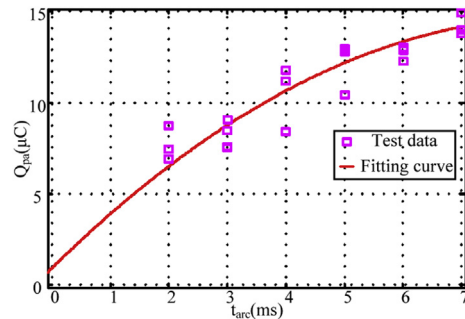


Fig. 7. The influence of the arcing time on the post-arc charge.

the residual charge at current-zero. The post arc charge is almost proportional to the residual charge in current-zero. The interaction between the arcing time and the post arc charge is useful to control the voltage distribution in multi-break VCBs with synergy control in our previous paper [14].

3.3. The influence of the current magnitude

When the arcing time and the TRV are 3 ms and 18 kV, and the main current is varied from 5 kA to 12.5 kA, the test is repeatedly conducted to gain the influence of the current magnitude on the post-arc charge. According to the Fig. 8, the distribution of the post-arc charge is almost constant when the current is from 5 kA to 12.5 kA. There may be some changes when the current is above 20 kA. However, the influence of the current magnitude is weaker than the arcing time. Therefore, the influence of the current magnitude on the post arc charge is little and can be neglected when the breaking current is less than 12.5 kA.

3.4. The relationship between the final position of the last cathode spot and the post-arc characteristic

The vacuum arc photos are observed by the high speed CMOS camera. The electrical measurements and the CMOS camera are in synchronously triggered by the synchronous controller. The photos of vacuum arc are observed when the current and the TRV are 10 kA and 22 kV respectively, which is shown in Fig. 8. In the Fig. 9 (a), the molten metal bridge becomes just before the contacts separate in 5.70 ms. The bridge ruptures as the contacts separate in 6.20 ms. The bridge column arc becomes in 8.55 ms and then transformed into diffuse vacuum arc in 10.05 ms. The distribution of cathode spots is uniform cross the surface in the vacuum arc extinguishing process between the 11.70 ms and the 11.95 ms. After a lot of interruption, the photos of vacuum arc are shown in Fig. 9 (b). The development of vacuum arc is different to the Fig. 9 (a) and the vacuum arc is concentrated on the right of the contacts. The final position of the last cathode spot is near the edge of the cathode surface.

The post-arc current and charge in the condition of the Fig. 9 (a) and (b) is shown in Fig. 10. The peak value of the post-arc current is 357 mA in the same condition of the Fig. 9 (b) while it is 643 mA in the condition of the Fig. 9 (a). In the same condition that the current and the TRV are 10 kA and 22 kV respectively, the post-arc current is absolutely different. The difference is the vacuum arc development and the final position of the last cathode spot. Therefore the post-arc current is closely related to the final position of the last cathode spot which is the result of the vacuum arcing memory. According to the post-arc current in Fig. 10 (a), the post arc charge is obtained, which is as shown in Fig. 10 (b). The final post arc charge

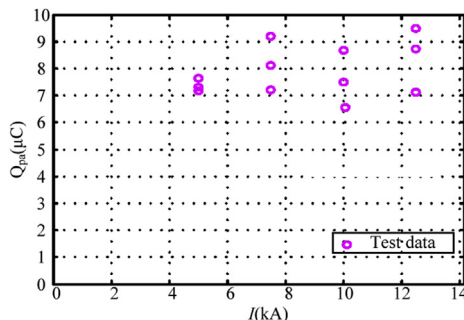


Fig. 8. The influence of the current magnitude on the post-arc charge.

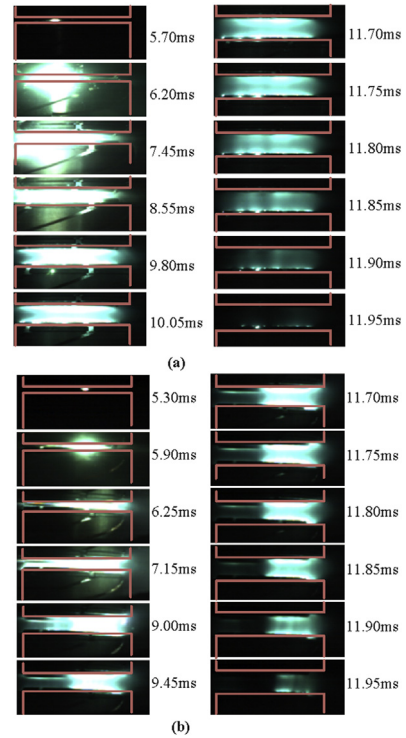


Fig. 9. Photos of the vacuum arc development.

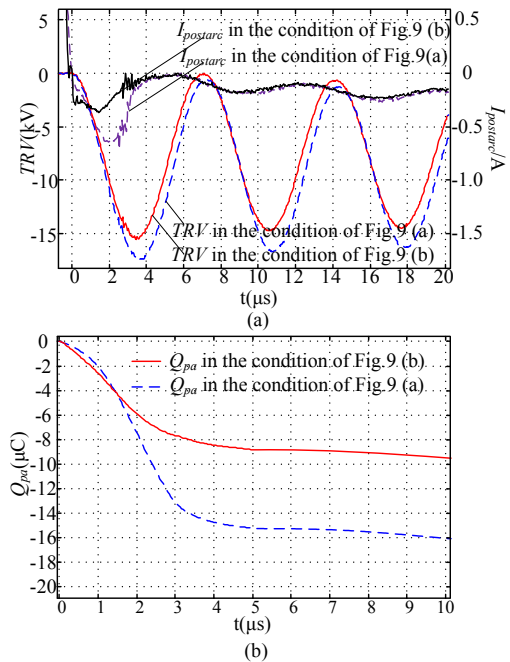


Fig. 10. Post-arc characteristic in the condition of Fig. 9 (a) and (b).

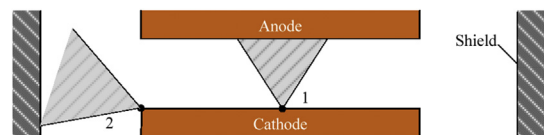


Fig. 11. The interaction between the final position and the residual plasma in current-zero.

in the condition of the Fig. 9 (a) and (b) is 16.0 μC and 9.7 μC respectively. When the final position of the last cathode spot is near the edge of the cathode surface in Fig. 9 (b), the post arc current and charge is less because that the residual charge in current-zero is ejected away from the contacts and absorbed by the vapour shield.

The interaction between the position and the residual plasma in current-zero is shown in Fig. 11. The cathode spots reduce as the arc current approaches zero. When the arc current reaches to zero, the final cathode spot extinguishes and the inter-electrode space contains residual plasma. The final position of the last cathode spot is the result of the arc memory which is the influence of the vacuum arc development on the current-zero characteristic. If the final cathode spot is extinguished at the centre of position 1, more charge returns to the anode than that of position 2. The residual plasma of the final cathode spot is ejected away from the cathode surface and absorbed by the vapour shield at position 2 while almost all of the residual plasma is returned to the electric circuits without considering the field emission and the neutralization at position 1. Therefore, post-arc characteristic is closely related to the final position of the last cathode spot.

4. Discussion

4.1. Influence of the magnetic field arc control on the current zero characteristic

The TMF forces the arc to rotate quickly across the surface of the contacts, thereby limiting the average thermal stress on it [3,17]. While AMF make the arc confined to the helices around the magnetic flux line so that the arc voltage can be stable and the arc remains diffused mode. The AMF has remarkably increased the breaking capacity of vacuum interrupters (VIs) than that of TMF and the post-arc current of VCBs with TMF is larger and more unstable [18,19]. In our previous researches [14], the influence of the AMF control on the post arc charge is investigated. The vacuum arc photos are observed by the high speed CMOS camera which is shown in Fig. 12. The main current and the TRV are 10 kA and 18 kV respectively. The externally applied AMF whose pulse width and magnitude is 10.0 ms and 50 mT is controlled in synchronization with the main current. In Fig. 12, the VCB contacts separates in 5.10 ms and the molten bridge becomes. Then the bridge ruptures in 5.30 ms and the vacuum arc column becomes in 5.75 ms. The vacuum arc transformed into diffuse mode in 7.85 ms. In the arcing time, the vacuum arc is uniform cross the cathode surface while the vacuum arc gradually extinguishes from 11.6 ms to 11.95 ms and vacuum arc is concentrates on centre of the inter-electrode. The

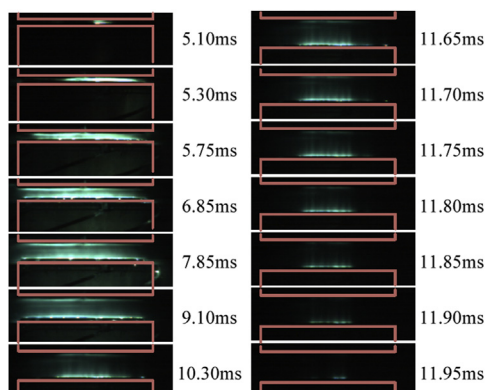


Fig. 12. Vacuum arc photos with external AMF control.

final position of the last cathode is in the centre of the cathode surface. Therefore, the AMF can make the vacuum arc diffuse and concentrated on the centre, so that the post arc current and charge is stable.

4.2. Demands of the current zero characteristic with multi-break VCBs

The voltage distribution of multi-break VCBs plays an important role on the breaking capacity [20,21]. Yanabu has investigated the relationship between the voltage distribution ratio and the post-arc current in double-break VCBs [22]. The unbalanced voltage is caused by the difference of the post-arc charge. In order to make the unbalance post arc charge, the AMF control is used. In addition, the synergy of the VCBs with double-break is that control the post-arc charge and the equivalent capacitance of VCBs [14]. According to the influence of the arcing time and the current magnitude on the post arc charge, the arcing time can be controlled to alter the post arc charge which is useful to the voltage distribution of multi-break VCBs.

5. Conclusion

The post-arc characteristic such as the post-arc current, conductance and charge is obtained by measuring and process the post-arc current. When TRV is 125 kHz, the valid duration of the post-arc characteristic will be below 4.8 μs ? The post-arc charge is more stable and smooth, so it is more optimal to describe the post-arc characteristic.

The post-arc charge can be used to describe the residual plasma at current zero and it is the effect of the arc memory. The post-arc charge increases as the arcing time increases and the influence of the current magnitude is weak when the current is from 5 kA to 15 kA.

Based on the photos of the vacuum arc, we can obtain that the post-arc characteristic is closely related to the final position of the last cathode spot. The relationship between the final position of the last cathode spot and the post-arc characteristic is gained and analyzed.

Acknowledgements

Project Supported by National Natural Science Foundation of China (51277020; 51477024; 51337001), Fundamental Research Funds for Central Universities (DUT13YQ102, DUT15ZD234).

References

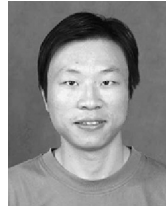
- [1] Power Circuit Breaker Theory and Design, 1st, 1982.
- [2] L. Min-fu, D. Xiong-ying, Z. Ji-yan, F. Xing-ming, S. Hui, Dielectric strength and statistical property of single and triple-break vacuum interrupters in series, IEEE Trans. Dielectr. Electr. Insul. 14 (3) (June 2007) 600–605.
- [3] P.G. Slade, The Vacuum Interrupter : Theory, Design, and Application, Crc Press, 2008.
- [4] E.P.A. van Lanen, The Current Interruption Process in Vacuum Analysis of the Currents and Voltages of Current-zero Measurements, TU Delft, Delft University of Technology, 2008.
- [5] J.G. Andrews, R.H. Valey, Sheath growth in a low pressure plasma, Phys. Fluids 14 (2) (June 1971) 339–343.
- [6] L.R. OramaExclusa, Numerical modeling of vacuum arc dynamics at current zero using atp, Proc. Int. Conf. Power Syst. Transients (Montreal, Canada on June 2005). Paper No. IPST05-155.
- [7] P. Sarrailh, L. Garrigues, G.J.M. Hagelaar, et al., Expanding sheath in a bounded plasma in the context of the post-arc phase of a vacuum arc, J. Phys. D Appl. Phys. 41 (1) (June 2007).
- [8] S. Rowe, et al., Post-arc period of vacuum circuit breakers: new 2D simulation and experimental results, in: Discharges and Electrical Insulation in Vacuum (ISDEIV), 2010 24th International Symposium on, Braunschweig, 2010, pp. 423–426.
- [9] Y. Mo, Z. Shi, S. Jia, et al., One-dimensional particle-in-cell simulation on the

- influence of electron and ion temperature on the sheath expansion process in the post-arc stage of vacuum circuit breaker, *Phys. Plasmas* 22 (no. 2) (2015).
- [10] A.V. Schneider, S.A. Popov, A.V. Batrakov, G. Sandolache, S.W. Rowe, Diagnostics of the cathode sheath expansion after current zero in a vacuum circuit breaker, *IEEE Trans. Plasma Sci.* 39 (6) (June 2011) 1349–1353.
- [11] A. KLAJN, Plasma parameters after forced switching off of the current in vacuum, *Przełąd Elektrotechniczny* 89 (9) (June 2013) 193–195.
- [12] K. Steinke, M. Lindmayer, Current zero behavior of vacuum interrupters with bipolar and quadrupolar AMF contacts, *IEEE Trans. Plasma Sci.* 31 (5) (Oct. 2003) 934–938.
- [13] E.F.J. Huber, K.D. Weltmann, K. Froehlich, Influence of interrupted current amplitude on the post-arc current and gap recovery after current zero-experiment and simulation, *IEEE Trans. Plasma Sci.* 27 (4) (Aug 1999) 930–937.
- [14] Guowei Ge, Minfu Liao, X. Duan, et al., Experimental investigation into the synergy of vacuum circuit breaker with double-break, *IEEE Trans. Plasma Sci.* 44 (1) (June 2016) 79–84.
- [15] Ge Guowei, Liao Minfu, X. Duan, et al., Methods of measuring post-arc current based on current transfer, *High. Volt. Eng.* 41 (9) (June 2015) 3156–3163.
- [16] G. Duning, M. Lindmayer, "Plasma density decay of vacuum discharges after current zero," *Discharges and Electrical Insulation in Vacuum*, 1998, in: *Proceedings ISDEIV.XVIIIth International Symposium on*, Eindhoven, vol. 2, 1998, pp. 447–454.
- [17] E. Schade, Physics of high-current interruption of vacuum circuit breakers, *IEEE Trans. Plasma Sci.* 33 (5) (Oct. 2005) 1564–1575.
- [18] S.M. Shkol'nik, et al., Distribution of cathode current density and breaking capacity of medium voltage vacuum interrupters with axial magnetic field, *IEEE Trans. Plasma Sci.* 33 (5) (Oct. 2005) 1511–1518.
- [19] N. Ide, O. Tanaka, S. Yanabu, S. Kaneko, S. Okabe, Y. Matsui, Interruption characteristics of double-break vacuum circuit breakers, *IEEE Trans. Dielectr. Electr. Insul.* 15 (4) (August 2008) 1065–1072.
- [20] M. Liao, X. Duan, X. Cheng, Z. Huang, J. Zou, Property of 126kV vacuum circuit breaker based on three 40.5kV fiber-controlled vacuum interrupter modules in series, in: *Discharges and Electrical Insulation in Vacuum (ISDEIV)*, 2012 25th International Symposium on, Tomsk, 2012, pp. 22–25.
- [21] G. Ge, M. Liao, X. Duan, S. Wang, X. Cheng, J. Zou, Experimental investigation on the matching characteristics of vacuum circuit breaker with double-break, in: *International Symposium on Discharges and Electrical Insulation in Vacuum (ISDEIV)*, Mumbai, 2014, pp. 493–496.
- [22] M. Sugita, et al., Relationship between the voltage distribution ratio and the

post arc current in double-break vacuum circuit breakers, *IEEE Trans. Plasma Sci.* 37 (8) (Aug. 2009) 1438–1445.



Guowei Ge was born in Henan, China, on September 18, 1987. He received the B.S. degree from Dalian University of Technology, Dalian, China, in 2013, where he is currently working toward the Ph.D. degree in the Department of Electrical and Electronics Engineering and is engaged in the study of vacuum switch with multi-break and intellectual apparatus.



Minfu Liao was born in Hunan, China, in 1975. He received the Ph.D. degree from Dalian University of Technology, Dalian, China, in 1999. He is currently a Professor with the College of Electrical and Electronic Engineering, Dalian University of Technology. He is engaged in the study of vacuum circuit breakers with multi-break and triggered vacuum switch.



Xiongying Duan was born in Hubei, China, on January 7, 1974. She received the B.S. and Ph.D. degrees in electrical power engineering from Huazhong University of Science and Technology, Wuhan, China, in 1996 and 2001 respectively. She is currently a Professor with the Department of Electrical and Electronics Engineering, Dalian University of Technology, Dalian, China. Her current research activities are concentrated on intelligent switching apparatus and electrical measurement technology.